Integrated interpretation of IP and TEM data for salinity monitoring of aquifers and soil in the coastal area of Muravera (Sardinia, Italy)

R. BALIA[1] AND A. VIEZZOLI[2]

[1] Dipartimento di Ingegneria Civile, Ambientale e Architettura, Università di Cagliari, Italy
[2] Aarhus Geofisica S.r.l., Polo Tecnologico di Navacchio (PI), Italy

ABSTRACT   The problem of aquifers and soil salinity is addressed in the coastal area of Muravera (SE Sardinia, Italy) with the combined use of electrical resistivity and induced polarization measurements along three lines, and with 41 Transient Electromagnetic (TEM) soundings distributed in the study area. The resistivity and chargeability sections provide a detailed information on the hydrogeological conditions in the first 20 - 60 m depth, clarifying the role of both clay and salt water and eventually confirming the local near-surface hydrogeological model. The resistivity maps obtained for different depth ranges by TEM data inversion, give a clear and effective representation of the saline contamination both laterally and down to a depth of about 70 m, over the whole investigated area. The combination of the geophysical techniques (resistivity tomography with Induced Polarization measurements, integrated with TEM soundings) proves very effective as an approach for soil and water salination monitoring.

Key words: coastal aquifers, salinization, groundwater monitoring, geophysical methods.

1. Introduction

Nowadays, the whole world is witnessing an increased pressure on groundwater resources, the main causes being population growth, socio-economic development, contamination, and climate change. In this context, coastal areas represent a particularly delicate hydrological setting, because of the presence of the transition zone between saline water and fresh groundwater. Exchanges of water masses occurring at this interface have a significant impact on the hydrological system since they can cause an increase in the salinity of the fresh groundwater, with obvious negative consequences on its availability, both for drinking and farming. On the other hand, a flow of fresh, but polluted groundwater into the saline groundwater, and then into the ocean, will affect the ecological system of the ocean itself.

Geophysical methods have been widely used for nonintrusive groundwater monitoring. Several case studies dealing with costal aquifers delineation were published in the last decades (e.g., Nowroozi et al., 1999; Yang et al., 1999; Shtivelman and Goldman, 2000; Choudhury et al., 2001; Balia et al., 2003, 2008; Manheim et al., 2004; Kafri and Goldman, 2005; Al-Garni and El-Kaliouby, 2011). Where present, the correlated problem of clay/saline groundwater having similar resistivity was either resolved with seismic measurements (Shtivelman and

Goldman, 2000; Choudhury *et al*., 2001; Balia *et al*., 2003), or with direct analysis of core samples/logs that allowed data calibration (Manheim *et al*., 2004; Kafri and Goldman, 2005), or it was not resolved at all (Nowroozi *et al*., 1999).

The application of Induced Polarization (IP) in environmental hydrogeology has seen a steep increase in the past fifteen years. However, most research focuses on groundwater contamination arising from surface sources (Aal *et al*., 2006; Martinho and Almeida, 2006; Sogade *et al*., 2006). Only in very few cases was IP applied in coastal areas with the purpose of hydrogeophysical modelling (Slater and Sandberg, 2000; Slater and Lesmes, 2002).

In this paper an approach to hydrogeophysical characterization of costal aquifers by integrating the resistivity, IP and Transient Electromagnetic (TEM) geophysical techniques is presented.

2. Experimental site and geophysical work

As experimental site, the coastal area of Muravera, south-eastern Sardinia Island, Italy, shown in Fig. 1, has been selected. It is crossed by the Flumendosa River, the island's second largest river, hence it is the terminal part of a fluvial valley including the river delta. The geology of the site and surrounding region is characterized, from bottom to top, by a Paleozoic complex cropping out on the edges of the plain, and Pleistocene and Holocene sediments and alluvium, up to a few hundred meters thick, covering the Paleozoic bedrock (Balia *et al*., 2003). Surface water bodies are the Flumendosa River, its channels at the river mouth (no longer connected with the river itself but which in the dry season contain incoming seawater), and several seasonal streams flowing from the surrounding hills. Apart from the water occurring in the fractured Paleozoic rocks, from which a few small ephemeral springs issue during the cooler months, groundwater is held primarily in the alluvial deposits. To date, based on hydrogeological and geophysical studies (e.g., Ardau and Barbieri, 1994; Ardau, 1995; Balia *et al*., 2003) as well as on numerous pits excavated and shallow drillings, two aquifers have been identified: a shallow phreatic aquifer extending down to a few tens of metres, and a deeper confined aquifer, separated from the former by a clayey layer, from a few to several tens of metres thick.

The natural hydrodynamic equilibrium between surface waters and fresh groundwater on the one hand, and the seawater on the other, is extremely critical in the Muravera coastal area. Apart from natural phenomena, such as recurrent drought, this equilibrium has been altered, since the 1950s, by upstream dams and river engineering works on the Flumendosa River, that have decreased the natural recharge of the coastal aquifers. The problem is compounded by an increasing uncontrolled exploitation of groundwater for irrigation in the summer. This has resulted in seawater intrusion and progressive groundwater and soil salination observed in the phreatic aquifer.

Groundwater quality monitoring over the last decades of the past century has produced evidence of seawater intrusion (Ardau, 1995). In particular, monitoring of the phreatic aquifer, which began in the 1980s (Barbieri and Barrocu, 1984; Ardau and Barbieri, 1994), has indicated the progressive advance of salination inland.

The area had already been the subject of geophysical studies with gravity, electrical
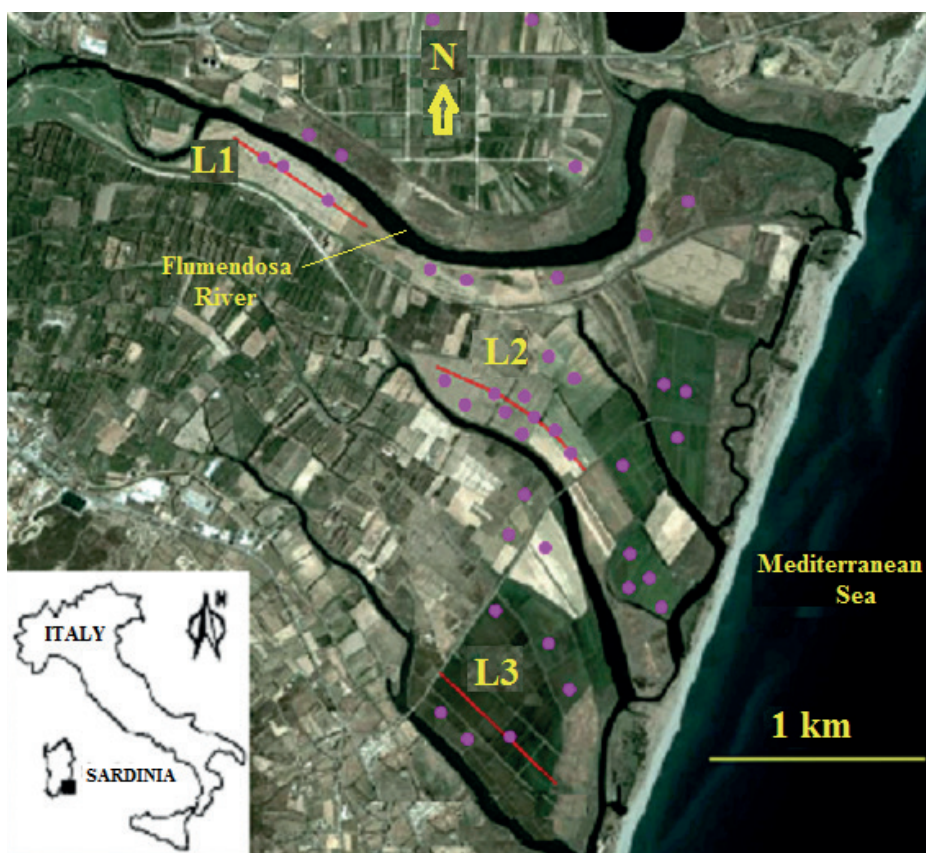
Fig. 1 - Plan view of the baseplate geometry used for the experiments. Transtension was produced by displacement of the plates 5° oblique to the principal displacement zones (PDZs). The stepover was underlain by a thin rubber membrane that stretched as the plates were displaced.

resistivity and reflection seismology surveys (Balia *et al.*, 2003) from which the hydrogeological model has been confirmed. However, while the use of integrated geophysical techniques proved to be very effective, the assessment of the actual extent of salination (both laterally and in depth) was not attained over the entire area. The agreement between the present results and those of the previous investigations is good for both the geophysical aspects and the consequent hydrogeological deductions.

As shown in Fig. 1, in the present work 41 TEM soundings and 3 lines for a total of about 2.1 km of resistivity and time domain IP measurements were acquired. For electromagnetic data acquisition, a WalkTEM instrument produced at the University of Aarhus, with a central square loop configuration (40 m side, loop area 1600 m^2), with 3 A current, turn-off time 4 μs, gate times from 10 μs to 10 ms was used; resistivity and IP data were acquired with a Wenner-Schlumberger configuration (minimum electrode spacing 2 m) by means of a modified multichannel ABEM system built at Lund University, with the receiver capable of sampling the IP decay at 50 Hz, recording the entire decay curve.

TEM data were processed and inverted with the SiTEM/Semdi software: it is an advanced program package for processing (SiTEM) and inversion (Semdi) of TEM data (http://www.aarhusgeo.com/). Electrical Resistivity Tomography (ERT) and IP data were

processed and inverted with a combination of Aarhus Workbench (http://hgg.au.dk/software/ aarhus-workbench/) and Res2dinv (http://www.geotomosoft.com/) programs. The normalized chargeability was also calculated following the approach of Lesmes and Frye (2001) in order to highlight the influence of lithological variations on the IP signatures. As also written by Lesmes and Frye (2001), the normalized chargeability, expressed as the ratio of chargeability to resistivity, is nothing but the specific capacity at first introduced by Keller (1959) and expressed in F/m.

As far as data inversion is concerned, the Mutually-Laterally Constrained Inversion (MCI-LCI) has been adopted. The joint inversion of different data sets is a popular research topic (e.g., Raiche *et al.*, 1985; Haber and Oldenburg, 1997; Wisén and Christiansen, 2005; Christiansen *et al.*, 2007; Vozoff and Jupp, 2007). As opposed to the other joint inversion procedures, the MCI-LCI allows a degree of flexibility between output models resulting from the different data sets, which reflects the different sensitivities and is governed by the width of the mutual constraints. This allows fitting the individual data sets while producing smooth models.

3. Results and hydrogeophysical interpretation

3.1. Resistivity and IP results

The resistivity and IP Line 1, the northernmost one, lies about 2.5 km from the seashore (Fig. 1) and extends for 700 m. The respective resistivity section (Fig. 2a) exhibits from top to bottom:

- a low resistivity (2 - 8 Ω·m) top horizon 5 - 10 m thick;
- an intermediate region, with increasing and relatively high resistivity (10 - 40 Ω·m), 20 - 30 m thick;
- decreasing resistivity (20 - 5 Ω·m) at the bottom.

The chargeability section (Fig. 2b) shows some IP response mainly at depths of 15 - 40 m, but some chargeability (Fig. 2c, normalized chargeability) can be appreciated also in the SE half of the section, at depths of 0 - 15 m.

Also referring to the general hydrogeological knowledge of the plain (Balia *et al.*, 2003 and references therein) the upper low-resistivity horizon, and the underlying with higher resistivity, can be respectively interpreted as two parts of a same geological layer extending down to a depth of about 30 - 35 m and constituted by fine-medium sand with variable silt and clay and minor pebbles. In the upper part, the resistivity is mainly governed by some clay and the salt deposited by brackish water which enters through the channels of the river and infiltrates laterally (where chargeability is low), by the salty spray conveyed inland by the sea wind and most likely from fertilizers used by farmers.

Conversely, the underlying horizon, belonging to the same geological layer but more resistive, hosts the shallow fresh aquifer, at least in the area corresponding to the central part of the section. The resistivity maximum between 100 and 200 m from the NW, very likely corresponds to the top of the Palaeozoic basement made up of metasandstones and metasiltstones with quartz veins, as found at a depth of 36 m in a borehole close to the north-western side of Line 1 [BH3 in Fig. 12, Balia *et al.*, (2003 of)]. On the SE of the section the chargeability indicates presence of polarizing materials at depths of 20 - 40 m, where resistivity is not very low (20 - 30 Ω·m): this could be due to some clay with fresh water.
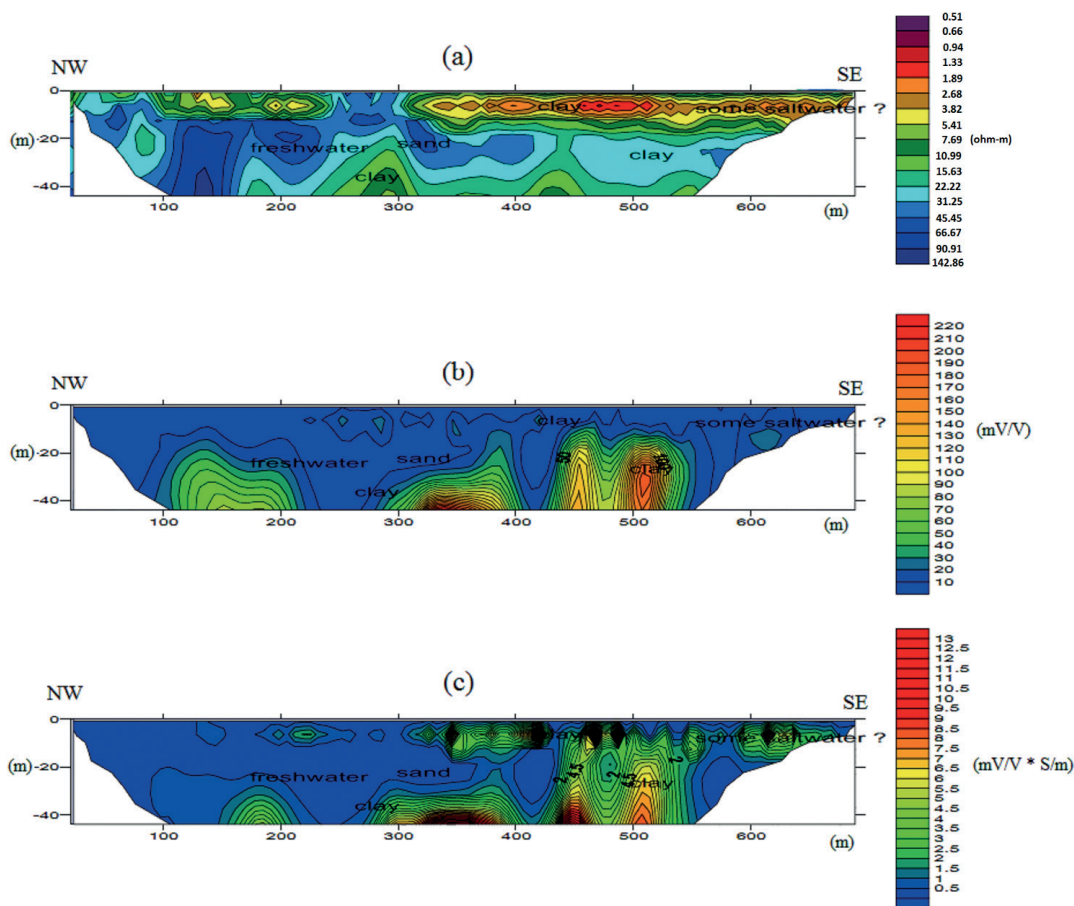
Fig. 2 - Resistivity (a), chargeability (b), and normalized chargeability (c) sections for line L1.

The resistivity section of Line 2 (Fig. 3) shows similar conditions, but the two horizons of the first layer are more clearly depicted:

- the top part of the surface layer, about 10 m thick, characterized by low resistivity (1 - 8 Ω·m) with near-surface origin as in the previous section;
- the deep part of the same layer hosting the shallow aquifer, with higher resistivity (15 - 45 Ω·m) due to reduced water salinity;
- the clayey layer which appears at depths of 30 - 40 m, with decreasing resistivity and increasing chargeability.

Along this line, the top layer should contain little clay, as indicated by the chargeability sections, and its low resistivity is mainly attributable to some brackish moisture and clay.

Fig. 4 shows the resistivity and IP sections for Line 3, which is the one closest to seashore. As can be seen, while the previous sections show information up to a depths of 40 and 60 m, in this case the maximum investigated depth is 20 m (thus referring just to the first layer) since deeper data were rather noisy, very likely due to current trapping in the shallow conductive layer. The highly conductive top horizon (1 - 3 Ω·m) has a thickness of the same order as in correspondence of the previous lines (10 - 12 m), but comparison with the chargeability sections indicates that the low resistivity is mainly due to saltwater, while clay should be very few. In the
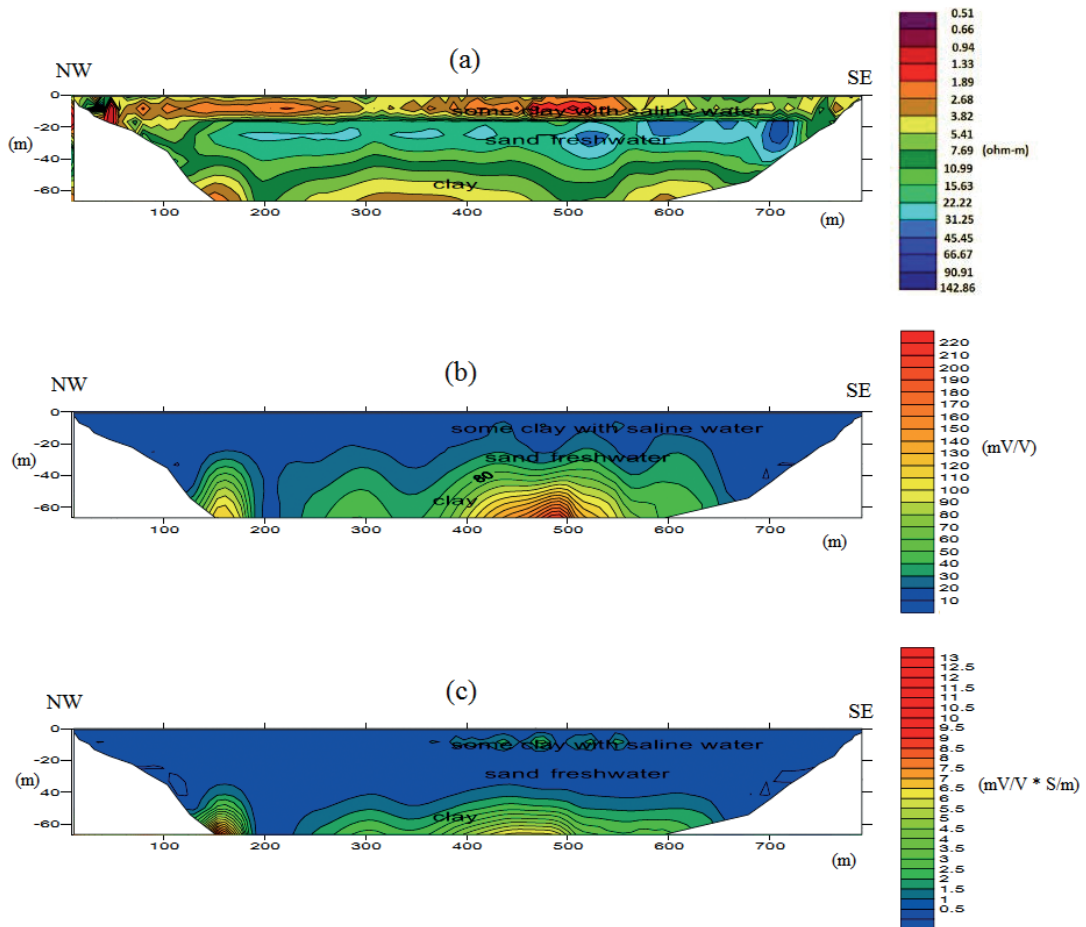
Fig. 3 - Resistivity (a), chargeability (b) and normalized chargeability (c) sections for line L2.

SE part of the section, 600 - 700 m from seashore, the freshwater seems disappear at all and be replaced by saltwater: this could be attributed to the sea water intrusion edge.

The localized zones of moderate chargeability in Figs. 4b and 4c at 100, 400 and 500 m, could be attributed just to locally increased clay.

The above results (IP and resistivity sections for Lines 1, 2 and 3) are in good agreement with the general hydrogeological model of the coastal plain and the results of previous hydrogeological and geophysical studies; however, if taken alone, these sections still do not provide a general view of salination, both laterally and in depth. The latter target will be achieved by means of the TEM measurements.

3.2. TEM results

First must be said that there was no indication of IP effects in the TEM data at the experimental site, due to the prevalently conductive nature of the subsurface in which the strong induced currents always prevail on the possible IP (displacement) currents.

The TEM data were edited to eliminate coupling to man-made structures and to increase the S/N ratio and, as said, were inverted to resistivity models using the SiTEM/Semdi software
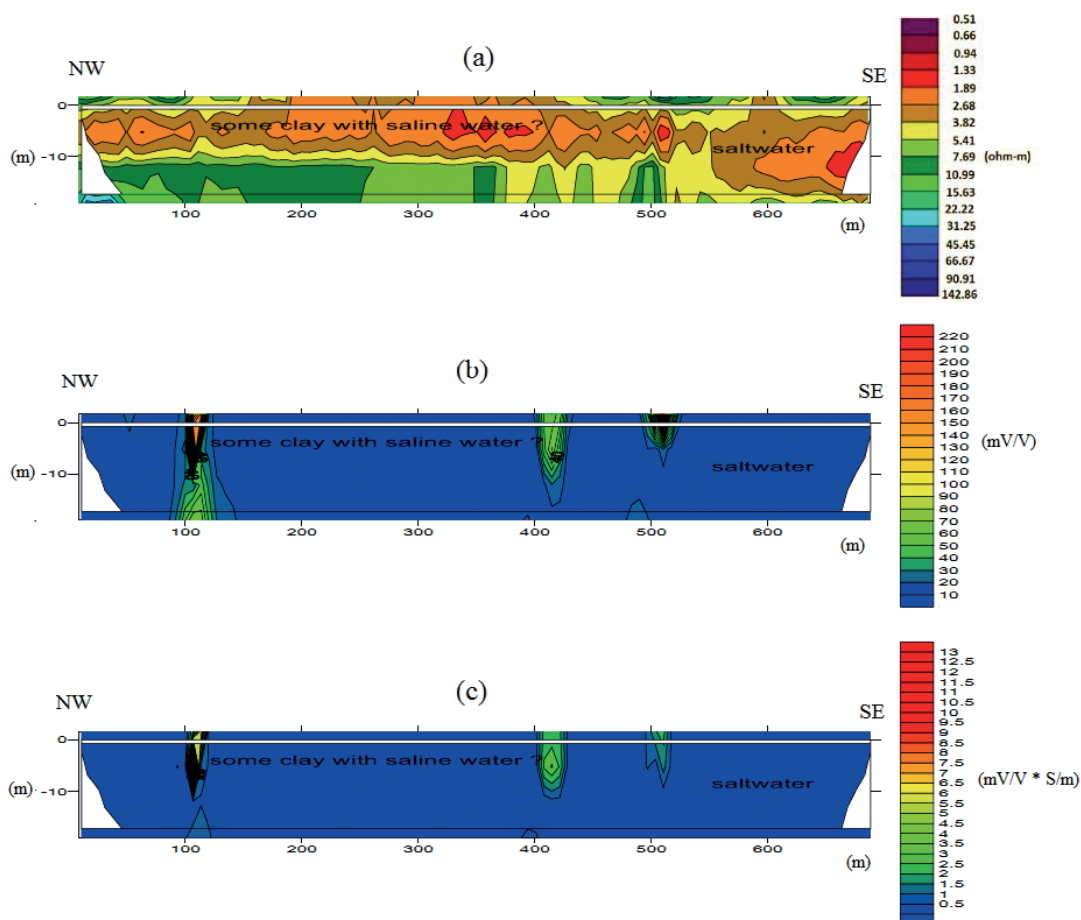
Fig. 4 - Resistivity (a), chargeability (b), and normalized chargeability (c) sections for line L3.

with the MCI approach. Then the resistivity columns have been processed to obtain several horizontal slices by means of a simple interpolation (inverse distance power 2), using a small, constant search radius allowing for some overlap across adjacent soundings, while avoiding excessive extrapolation. Each slice refers to a certain depth range and extends laterally over most of the survey area; these resistivity maps are shown in Figs. 5 to 7.

The four resistivity maps in Fig. 5 refer to depths of 0-5 / 5-10 / 10-15 / 15-20 m with respect to ground level. The first one (0-5 m) is fully representative of the widespread salinization of soils caused by lateral infiltration of brackish water from the river channels (phenomenon which mostly happens in the drought season when seawater is allowed to flow inland) and, equally relevant, caused by the saline aerosol carried by the sea wind, fertilizers and pesticides used by farmers. In other words, in the absence of lateral seepage of brackish water, saline aerosol, fertilizers and pesticides, this shallow portion (which is more or less wet but does not contain a true aquifer) would be characterized by a significantly greater resistivity, except for local presence of some clay. At depths of 5-10 m, the resistivity generally decreases due to both increasing salination and clay; the dependence of the resistivity decrease with respect to the proximity of the sea is clearly depicted.
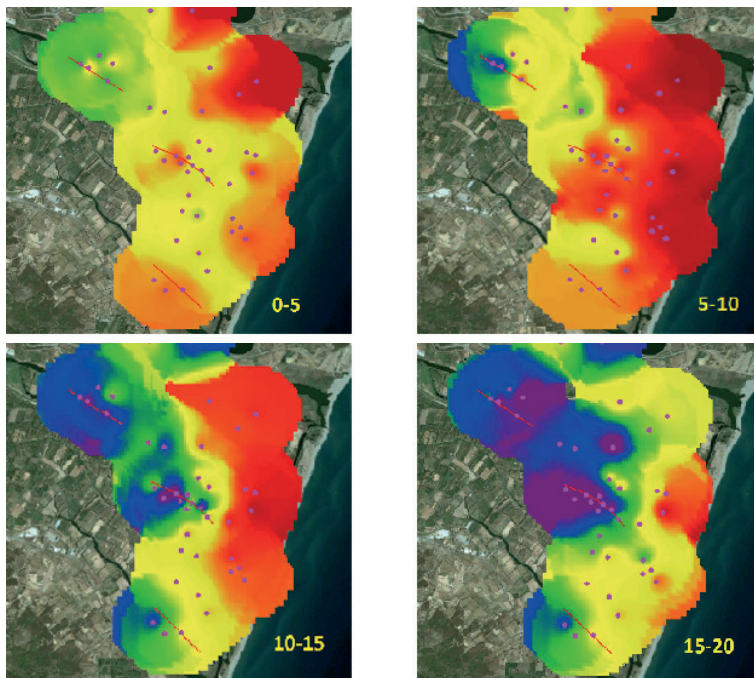
Fig. 5 - Electrical resistivity maps derived by TEM soundings at depth ranges of 0-5 / 5-10 / 10-15 / 15-20 m below ground surface.
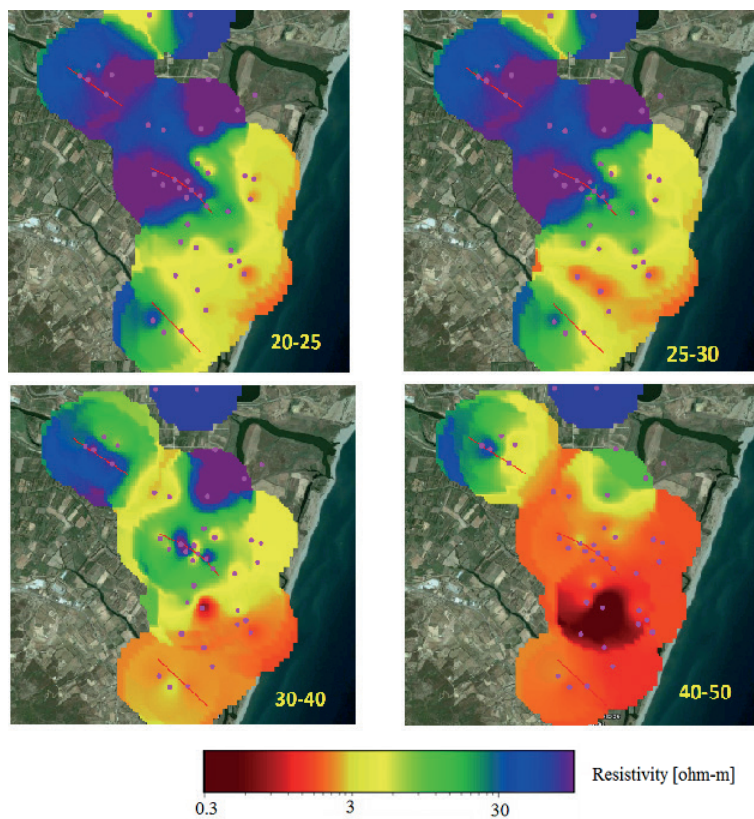
Fig. 6 - Electrical resistivity maps derived by TEM soundings at depth ranges of 20-25 / 25-30 / 30-40 / 40-50 m below ground surface.
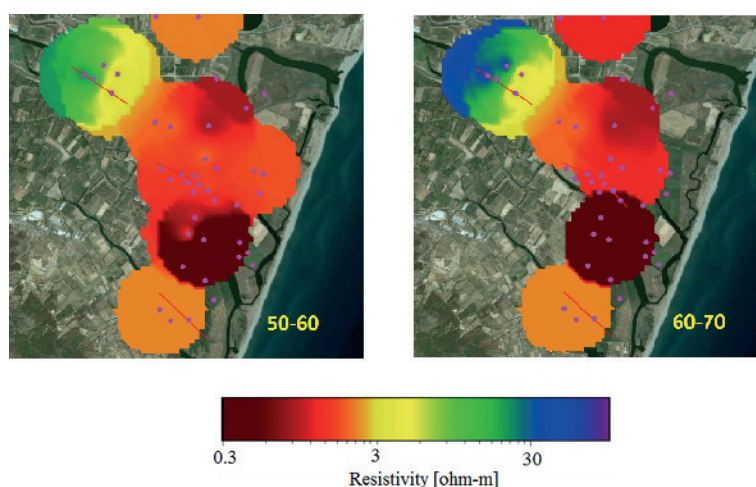
Fig. 7 - Electrical resistivity maps derived by TEM soundings at depth ranges of 50-60 / 60-70 m below ground surface.

At depths of 10-15 and 15-20 m (Fig. 5) the resistivity increases because the shallow freshwater aquifer appears, especially in the north-western sector; salinization decreases even in the near-seashore areas. This improvement reaches its maximum at depths of 20-25 and 25-30 m (Fig. 6): here, as well shown in the resistivity maps, the shallow freshwater aquifer (blue colour) reaches its maximum lateral extension; however, at depths of 25-30 m the beginning of a certain turnaround can be observed. In fact at depths of 30-40 m (Fig. 6) the lateral extension of the shallow freshwater aquifer is greatly reduced and the resistivity decreases significantly: this is mainly due to the clay layer (the one identified with the IP survey) which separates the shallow aquifer from the deeper one. Below depth of 40 m (Figs. 6 and 7) the salination spreads out abruptly and adds its effect to that of clay, as witnessed by the very low resistivity and drastic reduction of freshwater which can be found only in the extreme NW of the study area. This condition holds, even worst, at depths of 50-60 and 60-70 m (Fig. 7). However, at depths of 60-70 m freshwater reappears in the north-western sector and this is in good agreement with the resistivity section obtained by Balia *et al.* (2003) correlating resistivity columns from vertical electrical soundings along a line perpendicular to the seashore.

The survey at hand has been carried out in summer, just at the end of the dry season: it would be very interesting, for comparison, to repeat measurements immediately after the end of the wet season, when the river is full of fresh water.

4. Discussion and conclusion

The basic meaning in terms of hydrogeological model and salinization phenomena attributed to resistivity and IP results along the three lines (Lines 1, 2, and 3 in Figs. 2, 3, and 4) has been described in the previous section, as well as the meaning attributed to TEM results in the whole area. Some consideration must be done on the resistivity values provided by the ERT and the TEM soundings respectively. As said, the data have been inverted based on the criteria of LCI and MCI as illustrated for example by Christiansen *et al.* (2007), and the application
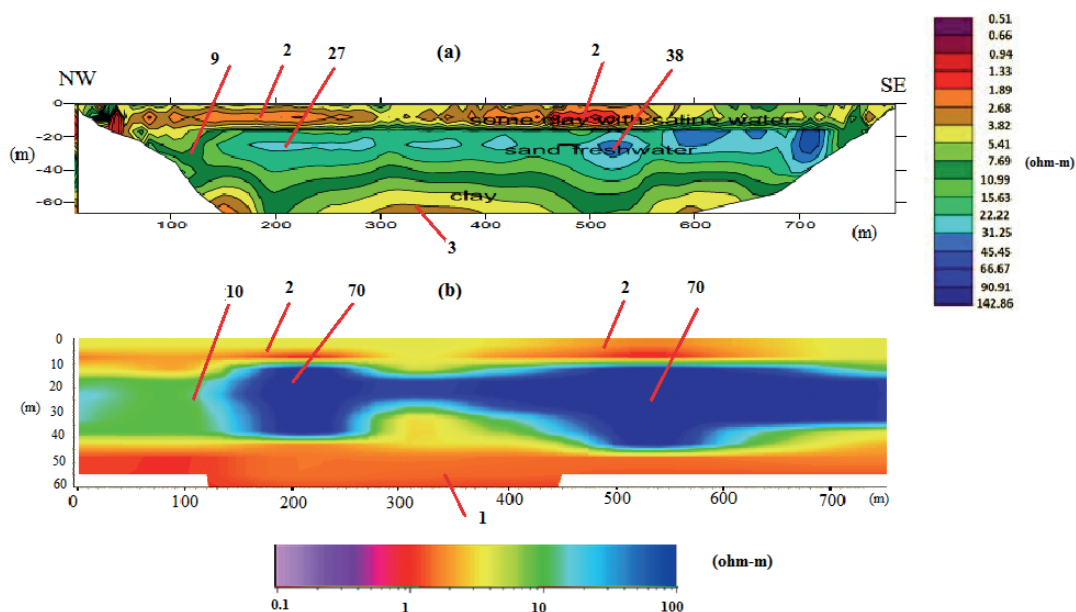
Fig. 8 - Comparison between the resistivity tomography for Line 2 (a) and the corresponding resistivity section from TEM data (b). Resistivity values are indicated for some comparison points.

of the above procedure has led to good lateral coherence between the two resistivity sets as concerns the sequence conductive - resistive - conductive and the thicknesses of the three electrical pseudo-layers. However, though the global misfit (normalized against noise) on the inversions of both TEM and ERT data was below 1, some, even important, differences can be noted between the resistivity values pertaining to the two techniques. This can be seen in Fig. 8 where, as an example, the ERT section for Line 2 is compared with the corresponding resistivity section obtained from TEM. The general agreement between the two sections is very good: the first unit with low resistivity, the intermediate one corresponding to the shallow aquifer with higher resistivity and, at the bottom, the low resistivity clayey layer. As for resistivity values, apart from very few discrepancies such as that in the NW part of Line 1 where the near surface resistivity provided by TEM is higher than that provided by ERT, the agreement in the low resistivity range (1 - 10 $\Omega \cdot$m) is good, while differences are substantial in the higher resistivity range, with values provided by TEM even doubled with respect to those provided by ERT. This can be attributed to several reasons, among which the substantially different underground volumes involved by the two techniques, and anisotropy phenomena. Looking at the positive aspects, in the TEM inverted data there is, at least in the case at hand, a significant enhancement of the resistivity contrast which results in a better resolution of the transitions from a more resistive to a less resistive layer and viceversa.

Summing up, the joint inversion of geophysical data and the subsequent joint interpretation of ERT, IP and TEM results, the latter performed along with the already acquired hydrogeological knowledge of the area, provide the following scheme:

1 - the area is characterized by a top sedimentary layer (Holocene alluvium, made up of silty-clayey soil and fine-coarse sand with rare pebbles) with a local thickness of about 30-40 m,

lying on a clay layer which separates the former from the underlying sediments. In this top sedimentary layer, two horizons can be clearly identified: the upper one, characterized by generally high salinity, and the lower one, which hosts a more or less freshwater phreatic aquifer;

2 - at distances less than 1 km from the sea, the upper horizon of the top layer, about 10-15 m thick, has a low resistivity due to clay and salt: the origin of the latter must be mainly attributed to near-surface transport mechanisms, such as lateral infiltration of seawater through the natural or man-made channels communicating with the sea, salt spray conveyed inland by the wind and fertilizers. Near the seashore the shallow aquifer, hosted in the lower horizon of the top layer, contains brackish-salt water, while at distances exceeding 1 km from the seashore it contains fresh water;

3 - at depths of 30-40 m, a clay-clayey layer constitutes the bottom of both the first layer and the shallow aquifer, and separates the latter from an underlying confined or semi-confined aquifer characterized by strong salination. The origin of this salination could be attributable to classical seawater intrusion or, most probably, to the fact that in a geological past the shoreline was about 2 km inland with respect to its present position (Barca *et al*., 1981);

4 - it is very likely that inland, particularly in the NW of the study area, there is no separation between the two aquifers or, rather, the only shallow aquifer exists, and lies directly on the Palaeozoic basement.

Based on the results of this study, under the methodological point of view it can be said that coupling IP and TEM proved to be an excellent tool and provided an information containing all details necessary for a good and independent hydrogeophysical interpretation. Actually, it must be also admitted that the good hydrogeological knowledge deriving from the previous studies has rendered easier the task of the hydrogeological interpretation of geophysical results. The great effectiveness and ease of interpretation of the resistivity maps sequence provided by TEM must be emphasized.

REFERENCES

Aal G., Slater L. and Atekwana E.; 2006: *Induced-polarization measurements on unconsolidated sediments from a site of active hydrocarbon biodegradation*. Geophys., **71**, H13–H24.

Al-Garni M. and El-Kaliouby H.; 2011: *Delineation of saline groundwater and sea water intrusion zones using Transient ElectroMagnetic (TEM) method, Wadi Thuwal area, Saudi Arabia*. Arabian J. Geosci., **4**, 655-668.

Ardau F.; 1995: *Studio dei fenomeni di salinazione delle acque sotterranee nella piana di Muravera (Sardegna sud-orientale)*. Ph.D. Thesis. in geologic-environmental engineering, VIII cycle, Politecnico di Torino, Università di Cagliari, Italy, 214 pp.

Ardau F. and Barbieri G.; 1994: *Evolution of phenomena of salt water intrusion in the coastal plain of Muravera (south-eastern Sardinia)*. In: Proc. 13th Salt Water Intrusion Meeting, Cagliari, Italy, Expanded Abstracts, pp. 305-312.

Balia R., Gavaudò E., Ardau F. and Ghiglieri G.; 2003: *Geophysical approach to the environmental study of a coastal plain*. Geophys., **68**, 1446-1459.

Balia R., Ardau F., Barrocu G., Gavaudò E. and Ranieri G.; 2008: *Assessment of the Capoterra coastal plain (southern Sardinia, Italy) by means of hydrogeological and geophysical studies*. Hydrogeol. J., **17**, 981-997.

Barbieri G. and Barrocu G.; 1984: *Consequences of overexploiting coastal aquifers in areas of touristic development in south-eastern Sardinia (Italy)*. In: Proc. Int. Conf. Water Resour. Plann. Manage., Athens, Greece, Expanded Abstracts, pp. 1-12.

Barca S., Di Gregorio F. and Palmerini V.; 1981: *Linea di costa pleistocenica nella piana di S. Priamo (Sardegna sud-orientale)*. Boll. Soc. Geol. It., **100**, 71-84.

Choudhury K., Saha D.K. and Chakraborty P.; 2001: *Geophysical study for saline water intrusion in coastal alluvial terrain*. J. Appl. Geophys., **46**, 189-200.

Christiansen A.V., Auken E., Foged N. and Sørensen K.I.; 2007: *Mutually and laterally constrained inversion of CVES and TEM data: a case study*. Near Surf. Geophys., **5**, 115-123.

Haber E. and Oldenburg D.; 1997: *Joint inversion: a structural approach*. Inverse Prob., **13**, 63-77.

Kafri U. and Goldman M.; 2005: *The use of the time domain electromagnetic method to delineate saline groundwater in granular carbonate aquifers and to evaluate their porosity*. J. Appl. Geophys., **57**, 167-178.

Keller G.V.; 1959: *Analysis of some electrical transient measurements on igneous, sedimentary and metamorphic rocks*. In: Wait J.R. (ed), Overvoltage Res. Geophys. Appl., Pergamon Press, New York, NY, USA, pp. 92-111.

Lesmes D.P. and Frye K.M.; 2001: *Influence of pore fluid chemistry on the complex conductivity and induced polarization responses of Berea sandstone*. J. Geophys. Res., **106**, 4079-4090.

Manheim F.T., Krantz D.E. and Bratton J.F.; 2004: *Studying ground water under Delmarva Coastal Bays using electrical resistivity*. Ground Water (Oceans issue), **42**, 1052-1068.

Martinho E. and Almeida F.; 2006: *3D behaviour of contamination in landfill sites using 2D resistivity/IP imaging: case studies in Portugal*. Environ. Geol., **49**, 1071-1078.

Nowroozi A.A., Horrocks S.B. and Henderson P.; 1999: *Saltwater intrusion into the freshwater aquifer in the eastern shore of Virginia: a reconnaissance electrical resistivity survey*. J. Appl. Geophys., **42**, 1-22.

Raiche A., Jupp D., Rutter H. and Vozoff K.; 1985: *The joint use of coincident loop transient electromagnetic and Schlumberger sounding to resolve layered structures*. Geophys., **50**, 1618-1627.

Shtivelman V. and Goldman M.; 2000: *Integration of shallow reflection seismics and time domain electromagnetics for detailed study of the coastal aquifer in the Nitzanim area of Israel*. J. Appl. Geophys., **44**, 197-215.

Slater L. and Sandberg S.; 2000: *Resistivity and induced polarization monitoring of salt transport under natural hydraulic gradients*. Geophys., **65**, 408-420.

Slater L. and Lesmes D.; 2002: I*P interpretation in environmental investigations*. Geophys., **67**, 77-88.

Sogade J., Scira-Scappuzzo F., Vichabian Y., Shi W., Rodi W., Lesmes D. and Morgan F.; 2006: *Induced-polarization detection and mapping of contaminant plumes*. Geophys., **71**, B75-B84.

Vozoff K. and Jupp D.L.B.; 2007: J*oint inversion of geophysical data*. Geophys. J. R. Astron. Soc., 4**2**, 977-991.

Wisén R. and Christiansen A.; 2005: *Laterally and mutually constrained inversion of surface wave seismic data and resistivity data*. J. Environ. Eng. Geophys., **10**, 251-262.

Yang C., Tong L. and Huang C.; 1999: *Combined application of dc and TEM to sea water intrusion mapping*. *Geophys*., **64**, 417-425.

Corresponding author: Roberto Balia
                            Dipartimento di Ingegneria Civile, Ambientale e Architettura, Università di Cagliari
                            Via Marengo 3, 09123 Cagliari, Italy
                            Phone: +39 070 6755170; fax: +39 070 6755033; e-mail: balia@unica.it